

Mechanism of Non-Capacitative Ca²⁺ Influx in Response to Bradykinin in Vascular Endothelial Cells

Pan-Cheung Leung^{a,b} Kwong-Tai Cheng^{a,b} Cuiling Liu^{a,b} Wing-Tai Cheung^c
Hiu-Yee Kwan^{a,b} Kin-Ling Lau^{a,b} Yu Huang^{a,b} Xiaoqiang Yao^{a,b}

^aLi Ka Shing Institute of Health Sciences, Faculty of Medicine, and Departments of ^bPhysiology and ^cBiochemistry, Chinese University of Hong Kong, Hong Kong, SAR, China

Key Words

Bradykinin · Diacylglycerol · Non-capacitative Ca²⁺ entry · Phospholipase C · TRPC6

Abstract

Bradykinin is a potent vasoactive nonapeptide. It elicits a rise in cytosolic Ca²⁺ (Ca²⁺)_i in endothelial cells, resulting in Ca²⁺-dependent synthesis and release of endothelial vasodilators. In the present study, we investigated the mechanism of bradykinin-induced Ca²⁺ influx in primary cultured rat aortic endothelial cells and in a mouse heart microvessel endothelial cell line (H5V). Bradykinin-induced Ca²⁺ influx was resolved into capacitative Ca²⁺ entry (CCE) and non-CCE. The non-CCE component was inhibited by a B2 receptor antagonist (HOE140; 1 μM) and a phospholipase C (PLC) inhibitor (U73122; 10 μM). The action of bradykinin could be mimicked by 1-oleoyl-2-acetyl-glycerol, an analogue of diacylglycerol (DAG), and by RHC80267, a DAG-lipase inhibitor. Immunoblots showed that TRPC6 was one of the main TRPC channels expressed in endothelial cells. Transfection of H5V cells with two siRNA constructs against TRPC6 both markedly reduced the TRPC6 protein level and, at the same time, decreased the percentage of cells displaying bradykinin-induced non-CCE. siRNA transfection also reduced the magnitude of non-CCE among the cells responding to bradykinin. Taken together,

our data suggest that bradykinin-induced non-CCE is mediated via the B2-PLC pathway, and that DAG may be involved in this process. Further, TRPC6 is one of the important channels participating in bradykinin-induced non-CCE in endothelial cells.

Copyright © 2006 S. Karger AG, Basel

Introduction

Bradykinin has pronounced beneficial effects on the cardiovascular system. It reduces the incidence of ventricular fibrillation, decreases postischemic reperfusion injuries in the heart, and exerts antihypertensive effect [1]. The beneficial effects of bradykinin have been mainly attributed to Ca²⁺-dependent synthesis and release of several endothelial mediators including nitric oxide, prostaglandins and endothelium-derived hyperpolarizing factors [1, 2].

Bradykinin evokes a biphasic elevation in endothelial cell [Ca²⁺]_i, an initial transient peak followed by a sustained plateau phase [3–5]. The initial transient rise is due to Ca²⁺ release from intracellular Ca²⁺ stores whereas the sustained phase is caused by extracellular Ca²⁺ entry through the plasma membrane [3, 4]. Upon binding to its receptor, bradykinin activates G-proteins G_{αi} and G_{αq}

[6], which in turn stimulate phospholipase C (PLC), leading to the generation of inositol 1,4,5-trisphosphate (InsP₃) and diacylglycerol (DAG) [7]. InsP₃ causes the Ca²⁺ release from the intracellular Ca²⁺ stores [8]. Resultant depletion of intracellular Ca²⁺ stores induces Ca²⁺ influx via capacitative Ca²⁺ entry (CCE) [8–10]. Bradykinin-induced CCE has been well studied in vascular endothelial cells [9, 10]. In addition to CCE, Ca²⁺ may enter the cells via non-CCE [11–13]. The mechanisms of activation for non-CCE appear to be diverse. Several common second messengers, e.g. InsP₃, inositol 1,3,4,5-tetrakisphosphate (InsP₄), DAG and arachidonic acid, have been found to activate Ca²⁺-permeable channels independent of Ca²⁺ store depletion [9, 11, 12, 14, 15]. Because bradykinin may stimulate the production of many of these second messengers, it is expected that bradykinin should be able to induce non-CCE. However, up to the present there are only a few studies investigating bradykinin-induced non-CCE in endothelial cells [16, 17]. The signal transduction pathways and ion channels that mediate bradykinin-induced non-CCE in endothelial cells are poorly defined.

TRPC channels are a group of Ca²⁺-permeable cation channels that may mediate CCE and non-CCE in endothelial cells [8, 18]. CCE is a common Ca²⁺ influx mechanism activated by diverse groups of Ca²⁺-mobilizing agonists [8]. In contrast, the activation mechanisms for non-CCE are diverse, and may differ with agonist types. It is possible that each agonist, through its unique signal transduction pathway, may activate specific TRPC subtypes to facilitate Ca²⁺ influx via non-CCE. Previous studies have demonstrated that basic fibroblast growth factor and vascular endothelial growth factor may evoke non-CCE by activating TRPC1 and TRPC6, respectively [19, 20]. For the non-CCE induced by bradykinin, Kamouchi et al. [17] overexpressed human TRPC3 in a bovine pulmonary artery endothelial cell line, which itself does not express endogenous TRPC3 channels. They found that the overexpressed TRPC3 was activated by bradykinin in a Ca²⁺ store-independent manner [17]. Up to the present, however, there are no available data showing the involvement of native endothelial TRPC channels in bradykinin-induced non-CCE.

In the present study, we investigated the bradykinin-induced Ca²⁺ influx in rat aortic endothelial cells and resolved the Ca²⁺ influx into CCE and non-CCE. Studies were also carried out to explore the signal transduction pathways and the endogenous TRPC channels involved in bradykinin-induced non-CCE.

Materials and Methods

Preparation and Culture of Rat Aortic Endothelial Cells and Mouse H5V Microvessel Endothelial Cells

All animal work was done in accordance with the Guide for the Care and Use of Laboratory Animals published by the US National Institutes of Health. Primary aortic endothelial cells were isolated and cultured as described elsewhere [21]. Briefly, the thoracic aortas were removed from male Sprague-Dawley rats of about 250–300 g. The aortas were cut open and treated with 0.25% collagenase in PBS for 15 min at 37°C. The suspension was centrifuged down and the cells were cultured in medium that contained 90% RPMI 1640 medium and 10% FBS. To avoid possible effects of culture conditions on endothelial cell properties, only cells of the first two passages maintained in culture condition for less than 1 week were used for experiments. The identity of the primary cultured rat aortic endothelial cells was examined by immunostains using an antibody against von Willebrand factor and the results showed that 98% of cells were of endothelial origin [21].

H5V cells, which were derived from murine embryonic heart microvessel endothelium transformed with polyoma middle-sized T antigen, were a generous gift from Dr. A. Vecchi, Italy [22]. The cells were grown in a culture medium that contained 90% DMEM and 10% FBS.

Measurement of Ca²⁺ and Mn²⁺ Influx

Ca²⁺ and Mn²⁺ influxes were measured either with the ratio-metric fluorescence Ca²⁺ dye Fura-2 using the PTI RatioMaster fluorescence system (Photon Technology International, Birmingham, N.J., USA) or with the single wavelength fluorescence dye Fluo-3 using the MRC-1000 laser scanning confocal imaging system. The endothelial cells were loaded with Fura-2/AM (10 μM) or Fluo-3/AM (10 μM) for 1 h in the dark at 37°C with 0.02% Pluronic F127 in culture medium. For Fura-2 fluorescence measurement, the Ca²⁺-bound and -unbound Fura-2 fluorescence signals were measured using dual excitation wavelengths at 340 and 380 nm. Average fluorescence values of 4–8 attached cells were recorded. These cells were mostly grown in separate regions with no apparent connection. Fluorescence ratios (R) were analyzed using the Felix program and were then used to calculate [Ca²⁺]_i as described by Grynkiewicz et al. [23]. Maximum (R_{max}) and minimum (R_{min}) fluorescence ratios of Fura-2 were determined by adding 10 μM of ionomycin in the presence of PBS containing 5 mM of CaCl₂, and in the presence of calcium-free physiological saline containing 5 mM of EGTA, respectively. The K_d of Fura-2 for Ca²⁺ was assumed to be 224 nM. For Fluo-3 fluorescence measurement, the excitation wavelength was at 488 nm. The data analysis was performed with the Confocal Assistant and MetaFluor. Changes in [Ca²⁺]_i in response to all agents were displayed as a ratio of fluorescence relative to the fluorescence, F₀, before the application of bradykinin.

Rat primary cultured aortic endothelial cells were transferred from culture medium to a Ca²⁺-free physiological saline solution (0Ca²⁺-PSS), which contained (in mM) 140 NaCl, 5 KCl, 2 EGTA, 1 MgCl₂, 10 glucose, and 5 Hepes, pH 7.4. Soon (2–3 min) after that, repetitive challenges of bradykinin (200 nM) were applied to deplete bradykinin-sensitive intracellular Ca²⁺ stores. CCE was then initiated by adding 2 mM CaCl₂ into the bath. Thapsigargin (4 μM), an endoplasmic reticulum Ca²⁺-pump inhibitor, was add-

ed 100 s prior to the induction of CCE to prevent Ca^{2+} from pumping back into intracellular Ca^{2+} stores during CCE.

After CCE reached its plateau, the cells were rechallenged with 50 nM bradykinin, 100 μM 1-oleoyl-2-acetyl-glycerol (OAG), or 50 μM RHC80267 to initiate non-CCE. In some experiments, 10 μM U73122, 10 μM U73343 or 1 μM HOE140 were added after repetitive bradykinin challenge but before the initiation of CCE.

H5V cells were treated with 4 μM thapsigargin for 30 min in normal physiological saline solution (NPSS) to deplete intracellular Ca^{2+} stores and to initiate CCE. Bradykinin (100 nM) was then added to elicit non-CCE. NPSS contained (in mM) 140 NaCl, 5 KCl, 1 CaCl_2 , 1 MgCl_2 , 10 glucose, and 5 Hepes, pH 7.4. For Mn^{2+} quenching experiments, immediately before the bradykinin (100 nM) challenge, the cells were transferred to Mn^{2+} -PSS, which contained (in mM) 140 NaCl, 5 KCl, 1 MnCl_2 , 1 MgCl_2 , 10 glucose, and 5 Hepes, pH 7.4.

siRNA and Transfection

We followed an siRNA strategy using vector-based inverted repeat sequence forming a hairpin structure in vivo [24]. A pair of inverted repeat sequences containing the 19-nt siRNA were synthesized for each siRNA. The sequences of the first pair (siRNA1) were: the strand 1, 5'-GTGTACAGAATGCAGCCAGTTC-AAGAGACTGGCTGCATTCTGTACACTTTTTT-3'; the strand 2, 5'-AATTAATAAAAGTGTACAGAATGCAGCCAGTCTCTTGAAGCTGGCTGCATTCTGTACACGGCC-3'. The second pair (siRNA2) sequences were: the strand 1, 5'-GTGTACAGAATGCAGCCAGTTCAAGAGACTGGCTGCATTCTGTACACTTTTT-3'; the strand 2, 5'-AATTAATAAAAGTGTACAGAATGCAGCCAGTCTCTTGAAGCTGGCTGCATTCTGTACACGGCC-3'. TRPC6-specific nucleotides are underlined. For each pair, two strands were annealed and then cloned into the self-constructed siRNA-expressing vector pcDU6C. pcDU6C was modified from pcDNA6 by substituting its CMV promoter with a U6 RNA polymerase III promoter. pcDU6C contained a blasticidin resistance gene for the selection of transfected eukaryotic cells and for the establishment of the stably transfected cell line. The insertion of siRNA-containing inverted repeat sequences into pcDU6C was verified by DNA sequencing. Both siRNA sequences were specific to TRPC6 only, and they will not cross-react with other TRPC isoforms.

H5V cells were transfected with either a siRNA-containing pcDU6C or an empty pcDU6C vector as a control using Lipofectamine 2000. Briefly, transfection was done with 4 μg of plasmid DNA and 6 μl of Lipofectamine 2000 in 200 μl of Opti-MEM-reduced serum medium in six-well plates, which contained $\sim 6 \times 10^4$ cells per well. After a 6-hour incubation at 37°C in a CO_2 incubator, Opti-MEM medium was removed and replaced by DMEM. Blasticidin (2 $\mu\text{g}/\text{ml}$) was added the next day and was maintained afterwards in culture medium. Under this selection pressure, the cell lines stably transfected with either the siRNA constructs or the control vector could be established in ~ 10 days.

SDS/PAGE and Immunoblots

Immunoblots were performed as described elsewhere [25]. Briefly, whole-cell lysates were extracted with protein extraction buffer, which contained 50 mM Tris-HCl, 150 mM NaCl, 1% Nonidet P-40, 0.1% SDS, 50 mM NaF, 2 mM EDTA, and 0.5% sodium deoxycholate, pH 7.5, with addition of complete protease inhibitor

cocktail tablets. Protein concentrations were determined by the Bradford assay (Bio-Rad). 100- μg proteins were loaded onto each lane and separated on an 8% SDS/PAGE gel after being boiled in SDS loading buffer. After electrophoresis, proteins were transferred to a PVDF membrane, and the membrane was then immersed in a blocking solution containing 5% non-fat milk and 0.1% Tween 20 in PBS buffer (140 mM NaCl, 3 mM KCl, and 25 mM Tris, pH 7.4) for 1 h at room temperature with constant shaking. The incubation with the primary anti-TRPC antibodies (1:200 dilution, Alomone Laboratories, Jerusalem, Israel) was carried out overnight in PBS buffer containing 5% non-fat milk and 0.1% Tween 20. Immunodetection was accomplished with horseradish peroxidase-conjugated secondary antibody, followed by the ECLTM Plus Western blotting detection system. Immunoblots with anti- β -tubulin antibody were used to confirm that an equal amount of proteins was loaded onto each lane. When needed, the intensity of the bands was analyzed by the FluorChem 8000 imaging system.

Materials

Fura-2/AM, Fluo-3/AM, and Pluronic F-127 were obtained from Molecular Probes, and RPMI 1640, DMEM, Opti-MEM, FBS, blasticidin, Lipofectamine 2000, and protease inhibitors were from Invitrogen. Primary antibodies against TRPC1, and TRPC3–6 were from Alomone Laboratories. Bradykinin, U73122, U73343, RHC80267, thapsigargin, cyclopiazonic acid, OAG and Bt_2 -InsP₄/AM were from Calbiochem. Nonidet P-40, sodium deoxycholate, SDS, EDTA, EGTA, collagenase type II, HOE140, CaCl_2 , Hepes, Tris-HCl and MgCl_2 were purchased from Sigma.

Results

Bradykinin-Induced Ca^{2+} Entry

Application of bradykinin (200 nM) onto the primary cultured rat aortic endothelial cells, which were bathed in 0Ca^{2+} -PSS, caused a transient rise in $[\text{Ca}^{2+}]_i$ (fig. 1), representing Ca^{2+} release from intracellular Ca^{2+} stores. After $[\text{Ca}^{2+}]_i$ returned to its basal level, 2 mM Ca^{2+} was added, which caused a rise in $[\text{Ca}^{2+}]_i$ (fig. 1). Similar results could be observed in H5V endothelial cells (data not shown). This $[\text{Ca}^{2+}]_i$ rise was due to Ca^{2+} influx, because it occurred immediately after the application of extracellular Ca^{2+} (fig. 1) and it could be inhibited by extracellular Ni^{2+} (3 mM; data not shown). Because the cells were bathed in 0Ca^{2+} -PSS for approximately 2–3 min before the bradykinin challenge and maintained there for about 10 min after the challenge, control experiments were performed to test whether the exposure to 0Ca^{2+} -PSS alone could lead to the subsequent Ca^{2+} influx in response to extracellular Ca^{2+} . In these control experiments, addition of 2 mM Ca^{2+} failed to increase $[\text{Ca}^{2+}]_i$ in the cells that had been exposed to 0Ca^{2+} -PSS for up to 30 min (data not shown), presumably because the exposure had not caused sufficient store depletion for CCE initiation.

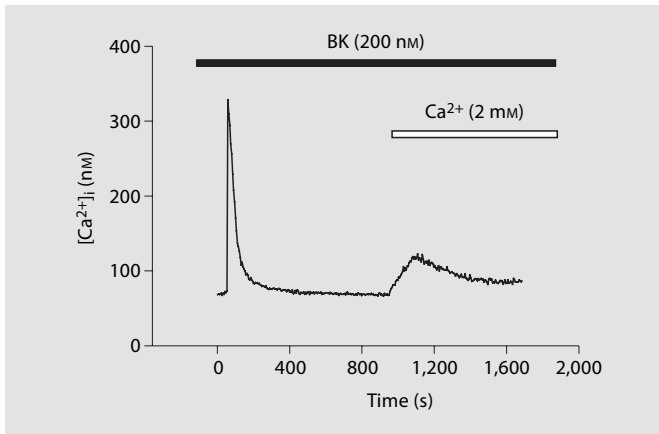


Fig. 1. Bradykinin-induced Ca^{2+} entry. A representative trace of Fura-2 fluorescence in rat aortic endothelial cells bathed in 0Ca^{2+} -PSS in response to bradykinin (200 nM) challenge. The trace represents the average fluorescence of 4–8 cells. $n = 6$ independent experiments.

In the continuous presence of bradykinin, both CCE and non-CCE could contribute to the Ca^{2+} influx. Therefore, a protocol was developed to resolve CCE and non-CCE. First, the cells bathed in 0Ca^{2+} -PSS were subjected to repetitive bradykinin challenges (200 nM) with a time interval of several minutes between each consecutive challenge until bradykinin failed to initiate any further $[\text{Ca}^{2+}]_i$ rise (fig. 2). 2 mM Ca^{2+} was then added to initiate CCE (fig. 2). After the CCE reached its plateau, bradykinin (50 nM) was applied and it elicited a further rise in $[\text{Ca}^{2+}]_i$ on top of the CCE (fig. 2). This $[\text{Ca}^{2+}]_i$ rise could not be attributed to intracellular Ca^{2+} release or CCE, because the bradykinin-sensitive Ca^{2+} stores were already emptied previously by a higher concentration of bradykinin (200 nM) and because the CCE had already reached a plateau. Therefore, we assigned this $[\text{Ca}^{2+}]_i$ rise as non-CCE (fig. 2). To confirm that ‘this non-CCE component’ was not due to residual Ca^{2+} release from stores, we performed control experiments using the same procedures as in figure 2 except that, immediately before the bradykinin (50 nM) challenge, the bath media were changed to 0Ca^{2+} -PSS. Subsequent bradykinin challenge failed to elicit a $[\text{Ca}^{2+}]_i$ rise, excluding the possibility of residual intracellular Ca^{2+} release. Note that we could not reject the possibility that ‘this non-CCE component’ could partly result from a reduced Ca^{2+} extrusion via $\text{Na}^+/\text{Ca}^{2+}$ exchanger in response to bradykinin. However, as will be

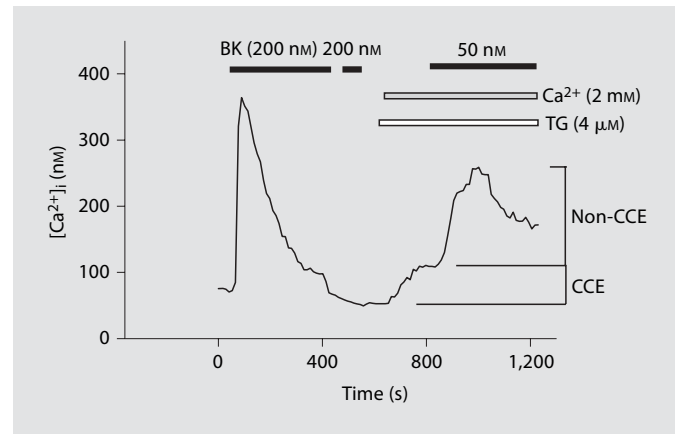


Fig. 2. Characterization of bradykinin-induced CCE and non-CCE in rat aortic endothelial cells. A representative trace of Fura-2 fluorescence showing bradykinin-induced CCE and non-CCE in rat aortic endothelial cells. Thapsigargin (TG, 4 μM) was added 100 s before the initiation of CCE to prevent Ca^{2+} from pumping back into intracellular Ca^{2+} stores. Duration of chemical treatments was shown as bars on top of the traces. $n = 9$ independent experiments.

described later, our data confirmed that this non-CCE was mostly due to Ca^{2+} influx via TRPC6 channels. We have not explored whether a change in membrane potential is involved in this bradykinin-induced non-CCE.

Signaling Pathways for Bradykinin-Induced Non-CCE

The selective B2 receptor antagonist HOE140 and the PLC inhibitor U73122 were used to study the signal transduction pathway of bradykinin-induced non-CCE in rat aortic endothelial cells. These cells were primary cultured cells that had not been subjected to prolonged cell culture conditions. Therefore, they may preserve the endothelial characteristics relatively well. Nevertheless, note that the cell isolation procedures itself could still result in some changes in cell properties. Hence, caution is still advised when trying to extrapolate the information obtained from primary isolated cells to in vivo tissues. HOE140 (1 μM) or U73122 (10 μM) was added after the completion of store depletion but 2 min before the initiation of CCE (application of 2 mM Ca^{2+}). Both HOE140 and U73122 greatly reduced the bradykinin-induced non-CCE (fig. 3a, b), whereas U73343 (10 μM), an inactive analogue of U73122, had no effect (fig. 3b). As expected, HOE140 and U73122 had no effect on the magnitude of CCE (fig. 3d, e), because these chemicals were applied after the completion of the store depletion process. These experiments clearly demonstrated that the non-

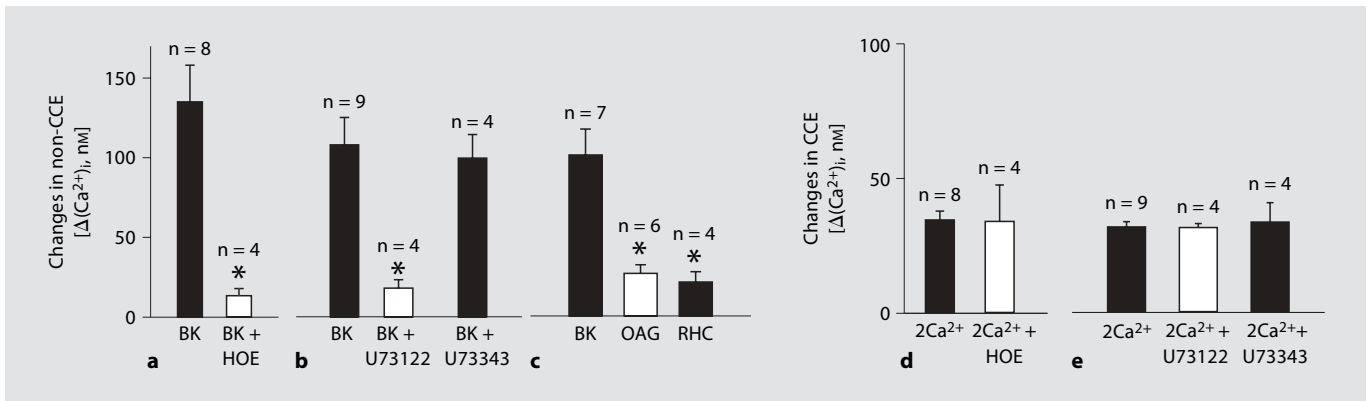


Fig. 3. Effect of HOE140, U73122, and U73343 on bradykinin (BK)-induced CCE, and the mimicking effect of OAG and RHC80267 on non-CCE. Experimental conditions were the same as in figure 2 except that HOE140 (1 μ M), U73122 (10 μ M) or U73343 (10 μ M) was added after the completion of store depletion but 2 min before the initiation of CCE. **a, b, d, e** Summary of the peak bradykinin-induced non-CCE (**a, b**) and CCE (**d, e**) in the absence or presence of HOE140 (1 μ M; **a, d**), U73122 (10 μ M; **b, e**)

or U73343 (10 μ M; **b, e**). Non-CCE was initiated by bradykinin (BK) (50 nM) whereas CCE was initiated by 2 mM Ca^{2+} . **c** Summary of the peak non-CCE in response to OAG (100 μ M), RHC80267 (50 μ M) or bradykinin (50 nM). Similar to bradykinin, OAG or RHC80267 was applied on top of the CCE plateau phase. Values are means \pm SEM of 4–12 independent experiments. * $p < 0.05$ vs. bradykinin alone.

CCE induced by bradykinin was mediated via the B2 receptor-PLC pathway.

PLC activity could generate multiple downstream products, such as DAG, $InsP_3$, and $InsP_4$. We tested the possible involvement of DAG and $InsP_4$. Similar to bradykinin, application of OAG, a membrane-permeant analogue of DAG, elicited non-CCE on top of the CCE plateau (fig. 3c). RHC80267 (50 μ M), a DAG-lipase inhibitor that prevents the breakdown of DAG, was also capable of eliciting the non-CCE (fig. 3c). However, the responses of cells to OAG or RHC80267 were much smaller than that to bradykinin (fig. 3c). We also tested the effect of Bt_2-InsP_4/AM , a membrane-permeant analogue of $InsP_4$, but Bt_2-InsP_4/AM (10 μ M) failed to elicit non-CCE.

Involvement of TRPC6 Channels in Bradykinin-Induced Non-CCE

Immunoblots were carried out to examine the expression pattern of TRPC channels in the rat aortic endothelial cells and H5V endothelial cells. Figure 4 shows that rat aortic endothelial cells expressed TRPC3, TRPC5 and TRPC6, and that H5V cells expressed TRPC4 and TRPC6. No expression was found for TRPC1 and TRPC4 in rat aortic endothelial cells, and TRPC1, TRPC3, and TRPC5 in H5V cells. The molecular weight of the rat TRPC3 band approximated 85 kDa, which may represent an alternatively spliced form reported previously [26]. The ex-

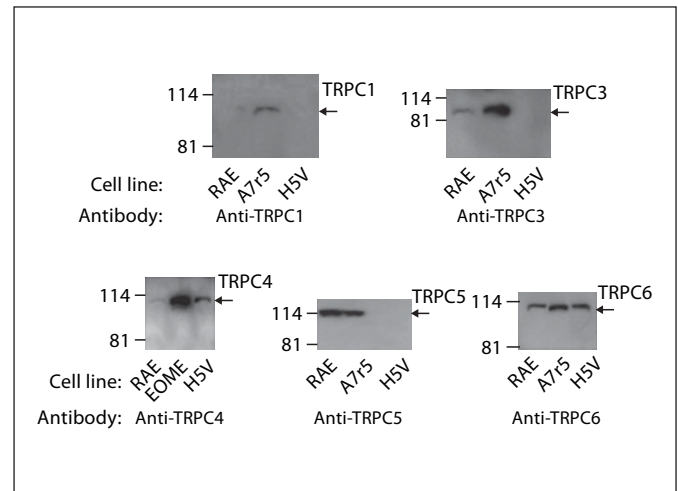


Fig. 4. Endogenous canonical transient receptor potential (TRPC) isoforms. Shown are representative immunoblots with antibodies against different TRPC isoforms ($n = 3$ for each experiment). Positive signals of expected molecular sizes were detected in the primary cultured rat aortic endothelial cells (RAE; TRPC3, 85 kDa; TRPC5, 111 kDa, and TRPC6, 107 kDa) and H5V cells (TRPC4, 112 kDa, and TRPC6, 107 kDa). No signal was observed for TRPC1 and TRPC4 in rat aortic endothelial cells, and TRPC1, TRPC3, and TRPC5 in H5V cells. Expressions in rat smooth muscle line A7r5 and mouse hemangioma-derived cell line EOMA were used as positive controls.

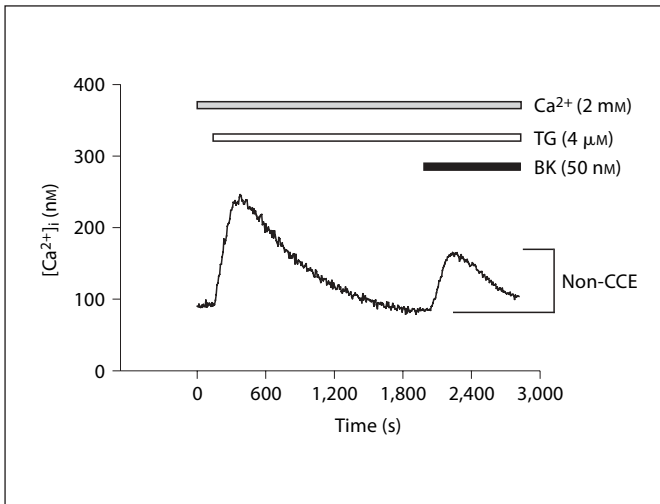


Fig. 5. Characterization of bradykinin (BK)-induced non-CCE in H5V endothelial cells. A representative trace of Fura-2 fluorescence showing bradykinin-induced non-CCE in H5V cells. Duration of chemical treatments was shown as bars on top of the traces. $n = 8$ independent experiments. TG = Thapsigargin.

pression of TRPC2 and TRPC7 was not examined due to the lack of commercial antibodies.

The siRNA strategy was used to study the functional importance of TRPC channels in bradykinin-induced non-CCE. Because of the difficulties associated with gene transfection in the primary cultured cells, we used the H5V cell line. Note that H5V endothelial cells were derived from mouse microvessels, whereas the rat aortic endothelial cells were isolated from aortas, i.e. large-sized arteries. Figure 5 shows that H5V cells preserve the property of bradykinin-induced non-CCE. Immunoblots indicated that TRPC6 is one of the most abundantly expressed TRPC channels in both the rat aortic endothelial cells and H5V cells (fig. 4).

A relatively simple protocol was developed to study the bradykinin-induced non-CCE in H5V cells. The cells were first treated with thapsigargin ($4 \mu\text{M}$) in NPSS for 30 min to deplete intracellular Ca^{2+} stores. Thapsigargin treatment caused a transient rise in $[\text{Ca}^{2+}]_i$ due to the release of Ca^{2+} stores and subsequent CCE, but the $[\text{Ca}^{2+}]_i$

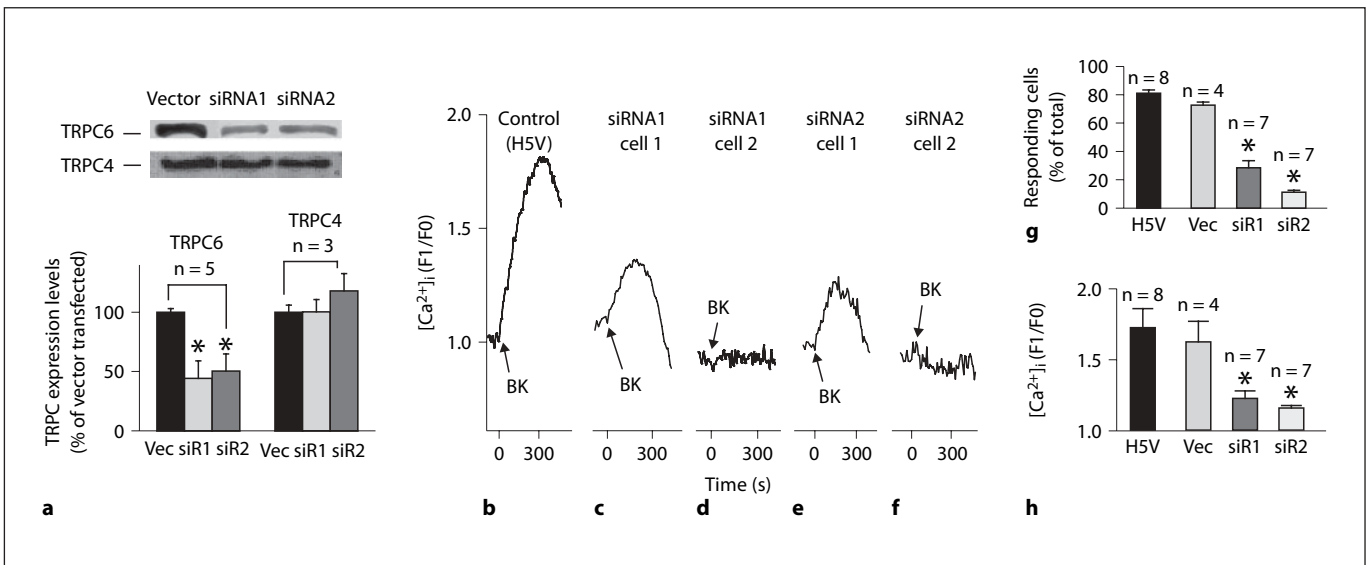


Fig. 6. Effect of siRNA constructs against TRPC6 on bradykinin-induced non-CCE in H5V cells. **a** Representative images (upper panel) and summary (lower panel) of immunoblot experiments. TRPC6 and TRPC4 expression levels were compared between siRNA-transfected H5V cells and the cells transfected with an empty vector. **b–f** Representative traces showing the non-CCE in response to bradykinin (100 nM) in non-transfected (**b**), siRNA1-transfected (**c**, a responding cell; **d**, a non-responding cell), and siRNA2-transfected H5V cells (**e**, a responding cell; **f**, a non-responding cell). Experimental procedures were the same as in figure 5 except that Fluo-3 fluorescence changes were measured.

Only the portion of experiments related to bradykinin-induced non-CCE is displayed. Changes in $[\text{Ca}^{2+}]_i$ were displayed as a ratio of fluorescence relative to the fluorescence level before the application of bradykinin ($\text{F1}/\text{F0}$). **g, h** Effect of siRNAs on the percentage of cells displaying bradykinin-induced non-CCE (**g**) and on the magnitude of peak non-CCE among the cells responding to bradykinin (**h**). Vec = Vector-transfected cells; siR1 = siRNA1-expressing cells; siR2 = siRNA2-expressing cells. Means \pm SEM (for **a**, $n = 5$ independent experiments; for **g, h**, $n = 4–8$ independent experiments, 15–40 cells per experiment). * $p < 0.01$ vs. non-transfected cells.

level approached basal levels within 15–20 min due to compensatory mechanisms from Na^+ - Ca^{2+} exchanger and plasma membrane Ca^{2+} -ATPase, which act to decrease the $[\text{Ca}^{2+}]_i$ level [27, 28] (fig. 5). After thapsigargin treatment, bradykinin (50 nM) was applied to elicit a further rise in $[\text{Ca}^{2+}]_i$ (fig. 5). We reasoned that, because the intracellular Ca^{2+} stores had been emptied by thapsigargin, bradykinin should not cause further intracellular Ca^{2+} release and CCE. Therefore, we assigned this component as non-CCE (fig. 5). Control experiments were performed to confirm the effectiveness of the thapsigargin treatment in emptying the intracellular Ca^{2+} stores. In these experiments, after the thapsigargin (4 μM) treatment for 30 min in NPSS, the cells were transferred to 0Ca^{2+} -PSS followed immediately by bradykinin challenge (50 nM). The bradykinin challenge failed to elicit a rise in $[\text{Ca}^{2+}]_i$, indicating that the stores were indeed emptied by thapsigargin treatment. Note that this protocol, in which thapsigargin was used to deplete the bradykinin-sensitive Ca^{2+} stores, is only suitable to H5V cells but not to rat aortic endothelial cells. In rat aortic endothelial cells, treatment of the cells with thapsigargin (4 μM) for 30 min failed to completely empty the bradykinin-sensitive Ca^{2+} stores.

Immunoblots show that siRNA constructs effectively reduced TRPC6 expression in H5V cells (fig. 6a). siRNA1 reduced the TRPC6 proteins by $57 \pm 10\%$ ($n = 5$) whereas siRNA2 decreased the TRPC6 proteins by $50 \pm 14\%$ ($n = 5$; fig. 6a). In control experiments, these siRNAs against TRPC6 had no effect on the expression of TRPC4 proteins (fig. 6a). Representative traces for bradykinin-induced non-CCE were shown for non-transfected H5V cells (fig. 6b), the cells transfected with siRNA1 (fig. 6c, d) and siRNA2 (fig. 6e, f). siRNAs markedly reduced the percentage of cells showing bradykinin-induced non-CCE. The non-CCE was observed in $81 \pm 2\%$ ($n = 8$) of non-transfected H5V cells and $73 \pm 2\%$ ($n = 4$) of vector-transfected cells (fig. 6g). The percentage was reduced to $28 \pm 5\%$ ($n = 7$) and $11 \pm 2\%$ ($n = 7$) in siRNA1- and siRNA2-transfected cells, respectively (fig. 6g). The siRNAs also decreased the magnitude of non-CCE among the responding cells. Among the cells displaying non-CCE, bradykinin increased the F1/F0 ratio to 1.72 ± 0.12 ($n = 8$) in non-transfected cells, and to 1.63 ± 0.12 ($n = 4$) in vector-transfected cells (fig. 6h). In siRNA1- and siRNA2-transfected cells, bradykinin only increased the F1/F0 ratio to $1.23 \pm 0.5\%$ ($n = 7$) and $1.16 \pm 0.2\%$ ($n = 7$), respectively (fig. 6h).

Alternatively, we also performed a Mg^{2+} quenching study to confirm the functional role of TRPC6 in brady-

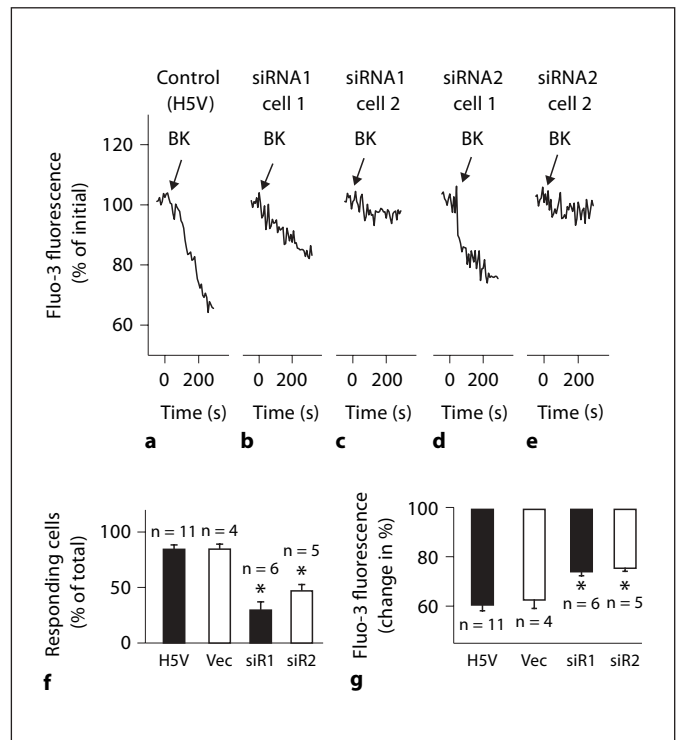


Fig. 7. Effect of siRNA constructs against TRPC6 on non-capacitative Mn^{2+} quenching in response to bradykinin in H5V cells. **a–e** Representative traces showing non-capacitative Mn^{2+} quenching in response to bradykinin (BK, 100 nM) in non-transfected (**a**), siRNA1-transfected (**b**, a responding cell; **c**, a non-responding cell), and siRNA2-transfected H5V cells (**d**, a responding cell; **e**, a non-responding cell). Experimental procedures were the same as in figure 6b except that immediately before the bradykinin challenge, the cells were transferred to Mn^{2+} -PSS. Only the portion of experiments related to bradykinin-induced non-capacitative Mn^{2+} quenching are displayed. **f, g** Effect of siRNAs on the percentage of cells displaying non-capacitative Mn^{2+} influx in response to bradykinin (**f**) and on the magnitude of Mn^{2+} influx among the cells responding to bradykinin (**g**). Means \pm SEM ($n = 4$ –11 independent experiments, 15–40 cells per experiment). * $p < 0.01$ vs. non-transfected cells.

kinin-induced non-CCE. Mn^{2+} is known to be a good substitute for Ca^{2+} in defining Ca^{2+} influx pathways. Because there is no intracellular Mn^{2+} store, the quenching reflects Mn^{2+} influx through the plasma membrane alone. In agreement with data in Ca^{2+} influx studies, both siRNAs decreased the percentage of cells displaying non-capacitative Mn^{2+} quenching in response to bradykinin (fig. 7a–f) and it also reduced the magnitude of non-capacitative Mn^{2+} quenching among the responding cells (fig. 7a–e, g).

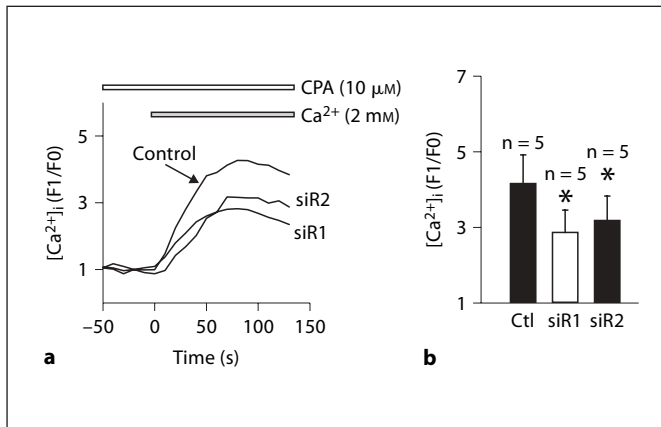


Fig. 8. Effect of siRNA constructs against TRPC6 on CCE in H5V cells. Cells transfected with or without siRNA-expressing constructs were treated with cyclopiazonic acid (CPA, 10 μ M) for 30 min in $0Ca^{2+}$ -PSS. 2 mM Ca^{2+} were then applied to initiate CCE. **a** Representative traces showing CCE. Only the portion of experiments showing CCE were displayed. **b** Summary of the data shown in **a**. Means \pm SEM (n = 5 independent experiments, 15–40 cells per experiment). Ctl = Control. * p < 0.05 vs. non-transfected cells.

At last, we examined the possible role of TRPC6 in CCE in H5V cells. Cells in $0Ca^{2+}$ -PSS were treated with cyclopiazonic acid (10 μ M) for 30 min to deplete intracellular Ca^{2+} stores. 2 mM Ca^{2+} were then applied to the bath to initiate CCE (fig. 8a). The results showed that the siRNAs against TRPC6 caused a small but significant reduction in the magnitude of CCE (fig. 8a, b), suggesting that TRPC6 is one of channels contributing to CCE in endothelial cells.

Discussion

B2 bradykinin receptor agonists are regarded as potential therapeutic medicines in the treatment of cardiovascular diseases like hypertension, cardiac hypertrophy, restenosis and myocardial infarction [1]. Beneficial effects of bradykinin receptor agonists on the cardiovascular system have been attributed to Ca^{2+} -dependent synthesis and release of several endothelial mediators [1, 2]. However, the mechanism of bradykinin-induced Ca^{2+} signaling in vascular endothelial cells, especially concerning the non-CCE component, is still poorly defined. In the present study, we examined the bradykinin-induced Ca^{2+} influx in rat aortic endothelial cells and resolved the Ca^{2+} influx into CCE and non-CCE. We found

that the bradykinin-induced non-CCE was mediated through B2 receptors and PLC. More importantly, we identified TRPC6 as one of the main channels mediating the bradykinin-induced non-CCE in endothelial cells.

One previous study by Huang et al. [16] has investigated the bradykinin-induced Ca^{2+} influx in canine corneal endothelial cells. The authors concluded that in these cells bradykinin induces Ca^{2+} influx independent of store depletion, and thus it appeared that only non-CCE could have accounted for the bradykinin-induced Ca^{2+} influx [16]. In the present study, we carefully designed the protocols and demonstrated that bradykinin can induce Ca^{2+} influx via both CCE and non-CCE. We believe that the discrepancy in results is at least partly due to inappropriate control in their report. Huang et al. [16] compared the bradykinin-induced Ca^{2+} influx between the cells with or without store depletion (using thapsigargin pretreatment for store depletion) and concluded that bradykinin-induced Ca^{2+} influx was not affected by the store depletion (with thapsigargin) [16]. However, in their control group, in which Ca^{2+} stores were not supposed to be depleted, agonist (bradykinin) was present, which would inevitably lead to store depletion. Presumably, that could lead to an inaccuracy in their conclusion.

Bradykinin may stimulate the activity of PLC [8], phospholipase A_2 [29] or phospholipase D [30], all of which may activate non-CCE [9, 12, 14, 15, 29, 30]. In the present study, U73122 treatment completely abolished bradykinin-induced non-CCE, suggesting a key role of the PLC pathway. We also attempted to identify the signaling molecules downstream to PLC, and found that OAG and RHC80267 could mimic bradykinin to initiate non-CCE. These results implicate a role of DAG in bradykinin-induced non-CCE. However, future experiments are needed to prove the involvement of DAG in bradykinin action, because a correlation between the inhibition of the DAG signal pathway and the reduction in bradykinin action is required. Of interest, the magnitude of non-CCE in response to OAG or RHC80267 was much smaller than that to bradykinin (fig. 3c), suggesting an involvement of other PLC downstream product(s) in addition to DAG. The possible involvement of $InsP_4$ was tested and excluded, but we did not test $InsP_3$ due to the lack of a membrane-permeant $InsP_3$ analogue.

Few studies investigating the involvement of endogenous TRPC channels in agonist-induced non-CCE in endothelial cells have been published. Among these, TRPC1 was found to be involved in non-CCE activated by basic fibroblast growth factor in bovine vascular endothelial cells [19], and TRPC6 was shown to be involved in non-

CCE activated by vascular endothelial growth factor in mesenteric artery endothelial cells in the rat and frog [20]. In the present study, we used siRNA technology to demonstrate that TRPC6 is one of main channels mediating bradykinin-induced non-CCE in vascular endothelial cells. This result is consistent with the finding that DAG, a known activator for TRPC6 [12], could activate non-CCE in endothelial cells (fig. 3c). In our experiments, however, both siRNA constructs could not completely abolish the bradykinin-induced non-CCE. This could either be due to incomplete 'knock-down' of TRPC6 proteins by the siRNAs or due to the participation of other channels in bradykinin-induced non-CCE. In agreement, H5V microvessel endothelial cells also express TRPC4 (fig. 4). A previous report has shown that TRPC5, a close relative of TRPC4, participates in bradykinin-induced non-CCE when overexpressed in pheochromocytoma PC12 cells [31].

In conclusion, this study provides the evidence that bradykinin can cause Ca^{2+} entry via both CCE and non-CCE in vascular endothelial cells. Bradykinin-induced non-CCE is mediated via the B2-PLC pathway, and DAG might be one of the PLC-downstream signaling molecules involved in the process. More importantly, TRPC6 is the main channel responsible for bradykinin-induced non-CCE in endothelial cells.

Acknowledgments

This study was supported by the Hong Kong Research Grant Council (CUHK4366/04M) and the Li Ka Shing Institute of Health Sciences (Chinese University of Hong Kong).

References

- Heitsch H: The therapeutic potential of bradykinin B2 receptor agonists in the treatment of cardiovascular disease. *Expert Opin Investig Drugs* 2003;12:759–770.
- Busse R, Fleming I: Molecular responses of endothelial tissue to kinins. *Diabetes* 1996; 45(suppl 1):S8–S13.
- Luckhoff A, Pohl U, Mulsch A, Busse R: Differential role of extra- and intracellular calcium in the release of EDRF and prostacyclin from cultured endothelial cells. *Br J Pharmacol* 1988;95:189–196.
- Morgan-Boyd R, Stewart JM, Vavrek RJ, Hassid A: Effects of bradykinin and angiotensin II on intracellular Ca^{2+} dynamics in endothelial cells. *Am J Physiol Cell Physiol* 1987;253:C588–C589.
- Schilling WP, Rajan L, Strobl-Jager E: Characterization of the bradykinin-stimulated calcium influx pathway of cultured vascular endothelial cells. Saturability, selectivity, and kinetics. *J Biol Chem* 1989;264:12838–12848.
- Liao JK, Homcy CJ: The G proteins of the G α i and G α q family couple the bradykinin receptor to the release of endothelium-derived relaxing factor. *J Clin Invest* 1993;92:168–172.
- Lambert TL, Kent RS, Whorton AR: Bradykinin stimulation of inositol polyphosphate production in porcine aortic endothelial cells. *J Biol Chem* 1986;261:15288–15293.
- Parekh AB, Putney JW Jr: Store-operated calcium channels. *Physiol Rev* 2005;85:757–810.
- Vaca L, Kunze DL: IP $_3$ -activated Ca^{2+} channels in the plasma membrane of cultured vascular endothelial cells. *Am J Physiol* 1995; 269:C733–C738.
- Vaca L, Kunze DL: Depletion of intracellular Ca^{2+} stores activates a Ca^{2+} -selective channel in vascular endothelium. *Am J Physiol* 1994;267:C920–C925.
- Barritt GJ: Receptor-activated Ca^{2+} inflow in animal cells: a variety of pathways tailored to meet different intracellular Ca^{2+} signaling requirements. *Biochem J* 1999;337:153–169.
- Hofmann T, Obukhov AG, Schaefer M, Harteneck C, Gudermann T, Schultz G: Direct activation of human TRPC6 and TRPC3 channels by diacylglycerol. *Nature* 1999;397: 259–263.
- Okada T, Shimizu S, Wakamori M, Maeda A, Kurosaki T, Takada N, Imoto K, Mori Y: Molecular cloning and functional characterization of a novel receptor-activated TRP Ca^{2+} channel from mouse brain. *J Biol Chem* 1998;273:10279–10287.
- Lückhoff A, Clapham DE: Inositol 1,3,4,5-tetrakisphosphate activates an endothelial Ca^{2+} -permeable channel. *Nature* 1992;355: 356–358.
- Mignen O, Shuttleworth TJ: I $_{ARC}$, a novel arachidonate-regulated, noncapacitative Ca^{2+} entry channel. *J Biol Chem* 2000;275:9114–9119.
- Huang SC, Chien C, Hsiao L, Wang C, Chiu C, Liang K, Yang C: Mechanisms of bradykinin-mediated Ca^{2+} signaling in canine cultured corneal epithelial cells. *Cell Signal* 2001;13:565–574.
- Kamouchi M, Philipp S, Flockerzi V, Wisenbach U, Mamin A, Raeymaekers L, Eggermont J, Droogmans G, Nilius B: Properties of heterologously expressed hTRP3 channels in bovine pulmonary artery endothelial cells. *J Physiol* 1999;518:345–358.
- Yao X, Garland CJ: Recent developments in vascular endothelial cell transient receptor potential channels. *Circ Res* 2005;97:853–863.
- Antonietti S, Lovisolo D, Fiorio Pla A, Munaron L: Expression and functional role of bTRPC1 channels in native endothelial cells. *FEBS Lett* 2002;510:189–195.
- Pocock TM, Foster RR, Bates DO: Evidence of a role for TRPC channels in VEGF-mediated increased vascular permeability in vivo. *Am J Physiol Heart Circ Physiol* 2004;286: H1015–H1026.
- Kwan HY, Huang Y, Yao X: Store-operated calcium entry in vascular endothelial cells is inhibited by cGMP via a protein kinase G-dependent mechanism. *J Biol Chem* 2000; 275:658–6763.
- Garlanda C, Parravicini C, Sironi M, De Rossi M, Wainstock de Calmanovici R, Carozzi F, Bussolino F, Colotta F, Mantovani A, Vecchi A: Progressive growth in immunodeficient mice and host cell recruitment by mouse endothelial cells transformed by polyoma middle-sized T antigen: implications for the pathogenesis of opportunistic vascular tumors. *Proc Natl Acad Sci USA* 1994;91:7291–7295.

- 23 Grynkiewicz G, Poenie M, Tsien RY: A new generation of Ca²⁺ indicators with greatly improved fluorescence properties. *J Biol Chem* 1985;260:3440–3450.
- 24 Brummelkamp TM, Bernard R, Agami R: A system for stable expression of short interfering RNAs in mammalian cells. *Science* 2002; 296:550–553.
- 25 Kwan HY, Huang Y, Yao X: Regulation of canonical transient receptor potential isoform 3 (TRPC3) channel by protein kinase G. *Proc Natl Acad Sci USA* 2004;101:2625–2630.
- 26 Ohki G, Miyoshi T, Murata M, Ishibashi K, Imai M, Suzuki M: A calcium-activated cation current by an alternatively spliced form of TRPC3 in the heart. *J Biol Chem* 2000;275: 39055–39060.
- 27 Kwan HY, Leung PC, Huang Y, Yao X: Depletion of intracellular Ca²⁺ stores sensitizes the flow-induced Ca²⁺ influx in rat endothelial cells. *Circ Res* 2003;92:286–292.
- 28 Goto Y, Miura M, Iijima T: Extrusion mechanism of intracellular Ca²⁺ in human aortic endothelial cells. *Eur J Pharmacol* 1996;314: 185–192.
- 29 Oike M, Droogmans G, Nilius B: Mechano-sensitive Ca²⁺ transients in endothelial cells from human umbilical vein. *Proc Natl Acad Sci USA* 1994;91:2940–2944.
- 30 Walter M, Tepel M, Nofer JR, Neusser M, Assmann G, Zidek W: Involvement of phospholipase D in store-operated calcium influx in vascular smooth muscle cells. *FEBS Lett* 2000;479:51–56.
- 31 Ohta T, Morishita M, Mori Y, Ito S: Ca²⁺ store-independent augmentation of [Ca²⁺]_i responses to G-protein coupled receptor activation in recombinantly TRPC5-expressed rat pheochromocytoma (PC12) cells. *Neurosci Lett* 2004;358:161–164.